Published in final edited form as:
Physica D. 2009 June 1; 238(11-12): 969–975. doi:10.1016/j.physd.2008.12.004.

Spontaneous onset of atrial fibrillation

Christian W. Zemlin, **Bogdan G. Mitrea**, and **Arkady M. Pertsov**
Department of Pharmacology, SUNY Upstate Medical University, Syracuse, New York 13210, USA

Abstract

Most commonly, atrial fibrillation is triggered by rapid bursts of electrical impulses originating in the myocardial sleeves of pulmonary veins (PVs). However, the nature of such bursts remains poorly understood. Here, we propose a mechanism of bursting consistent with the extensive empirical information about the electrophysiology of the PVs. The mechanism is essentially non-local and involves the spontaneous initiation of non-sustained spiral waves in the distal end of the muscle sleeves of the PVs. It reproduces the experimentally observed dynamics of the bursts, including their frequency, their intermittent character, and the unusual shape of the electrical signals in the pulmonary veins that are reminiscent of so-called early afterdepolarizations (EADs).

Keywords

cardiac arrhythmias; atrial fibrillation; pulmonary veins; spiral waves

Introduction

Atrial fibrillation (AF), the most common arrhythmia[1], is characterized by turbulence-like electrical activation of atrial tissue, leading to desynchronization of contraction. AF is not lethal, but those affected suffer a severe loss in quality of life2;3. Animal studies have shown that AF is initially paroxysmal4, i.e. it starts and terminates spontaneously, with episodes lasting less than a minute. Over time, AF episodes become longer[4] and eventually, chronic AF develops. In humans, the progression of AF from paroxysmal to persistent has also been observed[5].

The paroxysmal AF are triggered by bursts of electrical activity originating in the PVs and is often treated by thermally destroying a thin strip of tissue around the PVs (ablation) 6-9. Spontaneous bursting from the PVs in humans is preceded by a pause, i.e. a substantially prolonged resting period (diastolic interval), in two thirds of all bursting events10. This finding is in stark contrast to the experimental practice of AF induction, where rapid stimulation sequences are typically used. Figure 1A shows schematically the location of pulmonary veins in the heart. The PVs are located in the left atrium (see Panel A). In Panel B, we show an enlarged view of a single vein.

The finding that the PVs play a crucial role in AF initiation has provoked extensive research on their morphology and electrophysiology. This research revealed the existence of extended

Corresponding author: Dr. Christian Zemlin, Tel. +1-315-464-7988, Email: zemlinc@upstate.edu.

myocardial sleeves penetrating 5-20 mm deep into the vein11. Electrical conduction in these sleeves is significantly slowed down12;13. The rate of change of transmembrane voltage at the beginning of an action potential (upstroke velocity) in microelectrode recordings showed little change[13], suggesting that conduction slowing in the PVs is a result of reduced electrical coupling. The activation patterns in the myocardial sleeves are fractionated12 suggesting that electrical coupling is heterogeneous. Another characteristic feature of the PVs is spontaneous activity, which has been observed in PV tissue14-16 as well as in single myocytes isolated from PVs[17;18]. Yet, neither heterogeneous coupling nor automaticity have so far been implicated in the spontaneous onset of AF.

A finding that can be more directly linked to the spontaneous onset of AF is that stimulation of the vagal nerves can induce high-frequency bursts of electrical activity in isolated pulmonary veins19. This is remarkable since it seems to contradict best-known effect of vagal stimulation on the heart, the slowing of the heart rate20;21. It has been suggested that bursting is initiated by cells exhibiting pathological spontaneous oscillations at the end of their action potential, known as “early afterdepolarizations” (EADs)[19]. Indeed, electrical recordings similar to EADs have been reported during such bursts19. Paradoxically, the conditions that typically induce EADs, such as increased intracellular calcium concentration22 or a decrease in the potassium currents I_{Kr} or I_{Ks}[23;24] are not likely to occur during vagal stimulation.

In this paper, we present a computational model that provides a likely mechanism for the spontaneous onset of atrial fibrillation that is consistent with experimental observations. We show that a combination of slow pacemaker activity and non-uniform electrical coupling, characteristic for the pulmonary vein region, can lead to the spontaneous formation of non-sustained spiral wave reentry, inducing a rapid burst of electrical activation. According to this mechanism, the burst is triggered by a slowing of sinus rhythm (aka pause) caused by vagal stimulation which allows the ectopic pacemaker to fire and initiate a spiral wave. The observed EAD-like potentials are not a result of pathological changes of ionic properties of certain cells, but represent a non-local effect produced by a drifting spiral wave.

The Model

General tissue properties

In our study, we model an area of the myocardial sleeves of the pulmonary veins (see Figs. 1A and B). To simulate electrical propagation, we use standard reaction-diffusion equations:

$$\begin{aligned} C_m \frac{\partial V}{\partial t} &= -I_{ion}\left(V, \vec{x}\right) + \nabla \cdot (g \nabla V) \\ \frac{\partial \vec{x}}{\partial t} &= f\left(V, \vec{x}\right) \end{aligned} \tag{1}$$

where C_m is the specific capacitance of the cell membrane, V is the transmembrane voltage, I_{ion} is the total ionic current across the membrane, $\vec{x}$ is a vector containing all variables besides V that are used to describe the local state of the medium (including ion concentrations and gating variables), g is the local conductivity tensor, and f is a function describing the dynamics of all variables except for V. The ionic currents are modeled according to the canine atrial model of Ramirez et al.[25] To simulate pacemaker activity and the effects of vagal stimulation, the model was modified (see below). Figure 1D shows the action potential of this model. Equation 1 was solved on a domain of size 12 mm × 4 mm using a Euler scheme with a space step of 80 μm and a time step of 5 μs using a Beowulf cluster with 32 cores running at 2.4 GHz.

Boundary conditions

We used no-flux boundary conditions at all boundaries. In the context of the PV anatomy (Fig. 1B), the simulated patch can be interpreted as *one half* of a symmetrical 24×4 mm^2 circular band excised from a PV.

Conductivities

To simulate heterogeneous coupling we used a spatially non-uniform isotropic conductivity $g(x, y) = g_x(x, y) = g_y(x, y)$, where $g_x(x, y)$ and $g_y(x, y)$ are the local conductivities in x- and y-directions, respectively. Figure 1C illustrates the g we use: The conductivity is higher in the proximal part of the sleeve (closer to the atria, light grey) but lower in the distal part (closer to the lungs, medium grey). The transition between the two regions is sharp in the left part of Fig. 1C, but smooth in the right part. To describe such a transition analytically, we use a generic function describing a sigmoidal transition of varying steepness in two dimensions:

$$g_x(x,y) = g_y(x,y) = g_{\min} + \Delta g / \left(1 + e^{-k_y(x)(y-y_c)}\right)$$
$$k_y(x) = k_{y,0} + \Delta k_y / \left(1 + e^{-k_x(x-x_c)}\right),$$

where g_{min} is the minimum conductivity, Δg is the difference between maximum and minimum conductivity, $k_y(x)$ characterizes the steepness of the transition from lower to higher conductivity in y-direction, and k_x describes how abruptly that steepness changes in x-direction.

The standard values used in our simulations where: g_{min} = 0.108 S/m, g_{max} = 0.81 S/m, k_x = 1/mm, $k_{y,0}$ = 0.25/mm, Δk_y = 99.75/mm x_c = 10 mm, and y_c = 2 mm. These values yield propagation speeds of about 30 cm/s in the proximal part and 10 cm/s in the distal part of the myocardial sleeves, well within the range observed in experiments[13]. The parameters k_x, $k_{y,0}$ and Δk_y have been chosen to reproduce the fractionated propagation in the PV region that has been reported in experiments[12;13].

Spontaneous activity

To simulate ectopic spontaneous activity, we designed an "ectopic pacemaker region" (a square of $l_p \times l_p$ cells), in which we eliminated the (outward) current I_{k1}, and increased the (inward) calcium current I_{Ca} (10-fold) and reduced electrical coupling with the surrounding non-pacemaking tissue. The changes in I_{k1} and I_{Ca} are sufficient to produce spontaneous activity in an isolated tissue patch, however, the activity disappears when the pacemaker is strongly coupled to the surrounding tissue. To achieve propagation from the pacemaker region to the rest of the tissue, we reduced the coupling g in the pacemaker region, thus lowering the electrotonic drain due to surrounding non-pacemaker cells. The reduction of coupling was implemented by multiplying $g(x,y)$ with a factor $p(x,y)$ in the pacemaker region. The factor $p(x,y)$ is given by

$$p(x,y) = p_0 + (1 - p_0)\frac{\sqrt{\left(x - x_p\right)^2 + \left(y - y_p\right)^2}}{\sqrt{2} l_p},$$

where x_p and y_p are the coordinates of the pacemaker. It can be seen that p has the value p_0 at the center of the pacemaker ($p_0 \approx 0$) and the value 1 at the periphery of the pacemaker, where $x\text{-}x_p = y\text{-}y_p = l_p$. The values we used in our simulations are p_0=0.13 and l_p = 9 pixels, which was sufficient to produce stable, ectopic activity in the absence of sinoatrial pacing.

Figure 1D shows action potentials of myocytes. The action potential of normal atrial cells (Sub-panel a) is characterized by a pronounced initial spike and a duration of about 200 ms. The pacemaker action potential (Sub-panel b), due to the absence of I_{k1} and the increased I_{Ca}, exhibits spontaneous depolarization (as seen at the end of the trace) and a prolonged duration.

Spatially variable ion channel densities

It has been reported that the ionic current densities in the distal PV can differ from those of atrial cells as follows[26]: I_{K1} is reduced by 58%, I_{to} by 25% and $I_{Ca,L}$ by 30%, while I_{Ks} and I_{Kr} are increased by 25% and 30%, respectively. To study the effect such differences, we used the above current densities for the distal pulmonary veins and varied the ionic current densities linearly along the *y*-axis.

Vagal stimulation

Vagal stimulation affects cardiac electrophysiology by modulating ACh-sensitive channels[27], and the modulation can with good accuracy be modeled by changing the amplitude of the I_{k1} current[28]. To simulate vagal activation, we doubled the standard I_{k1}. Figure 1D, Subpanel c) shows an action potential of a myocardial cell with vagal stimulation modeled as described above. The increased (outward) I_{k1} reduces the action potential duration to about 100 ms, which is in good agreement with the effect of vagal stimulation determined experimentally for moderate vagal stimulation[29].

Sinus beats

In order to reproduce the spontaneous onset of AF realistically, we simulated the invasion of sinus waves into the PV area. To initiate the arrival of a sinus beat, we stimulated the whole proximal edge of the modeled region by applying 2 ms current pulses with twice the excitation threshold. The effect of vagal stimulation on sinus rhythm was modeled by a reduction of the pacing rate.

Results

Our studies show that a latent pacemaker in the vicinity of heterogeneities in electrical coupling can trigger intermittent spiral wave formation giving rise to a bursting pattern as observed in PVs during AF. The mechanism of such bursting is illustrated in Fig. 2. Panel A shows the activation of the PV region by a sinus beat before the onset of bursting. The normal sinus wave (entering the PV from the atria) propagates from the bottom to top. While there is an endogenous pacemaker in the upper left corner of the medium, it does not fire, because it is reset by the sinus wave before it can generate an activation itself.

The bursting is triggered by spontaneous reduction of the heart rate, below that of the latent pacemaker. In the real heart, such a reduction can be the result of vagal stimulation. As a consequence of a pause, the next activation (see Panel B) originates not from the atria, but from the endogenous latent pacemaker. The wave generated by the latent pacemaker propagates to the right, but is prevented from propagating downwards into the high-conductivity region by a sharp conductivity gradient. Such a block is a result of impedance mismatch when the current generated in at the propagating front in the high impedance area (purely coupled cells) is insufficient to raise potential above excitation threshold in the low impedance area (well-coupled cells). The surviving fragment of the wave (see Fig. 2B) continues to propagate to the right until it reaches the right boundary of the medium, where the conductivity gradient in *y*-direction is smoother and downwards propagation is possible (see Panel C). As the wave propagates downward, it collides with the next sinus wave, annihilating the right part of the sinus wave. The left part of the sinus wave survives and reenters into the upper half of the medium, producing a spiral wave (see Panel D). The spiral wave is not stationary but drifts to

the right along the sharp transition in conductivity (compare Panels D, E and F); this drift is caused by the coupling gradient. After reaching the right end of the sharp transition of conductivity, the spiral wave drifts to the upper boundary and disappears (not shown).

The bursting frequency equals the reentry frequency of the spiral wave (~ 8 Hz). The burst duration equals the lifetime of the drifting spiral, which was 6 rotations in this simulation. In a large set of simulations, we observed burst durations from 2-8 activations. Subsequently, the pacemaker recovers, and if the sinus rate remains low, it again has the chance to fire and to induce another spiral wave giving rise to another burst.

The burst dynamics are most apparent in the electrical recordings from individual tissue locations (Panels a-c). Trace (a) shows the transmembrane signal from a cell inside the pacemaker region. The first three excitations are caused by sinus rhythm. The fourth activation is initiated by the pacemaker, and the subsequent three excitations are caused by a spiral wave. After these three excitations, the spiral has drifted out of the medium, so that the next excitation comes from the pacemaker, which again induces a spiral wave that produces three more activations. This sequence of pacemaker beats initiating spirals continues for as long as the sinus frequency is lower than the natural frequency of the pacemaker.

Trace (b) shows the transmembrane signal from a cell in the normally conducting region. Again, the first three beats are driven by the sinus rhythm. Then, after a longer interbeat interval, arrives the first pacemaker ectopic beat. The pause is 180 ms longer than in trace (a), reflecting the time it takes for the abnormal beat to travel around the line of block (see Panels B and C). The ectopic beat is followed by a burst of six pulses, which correspond to the activity of a spiral wave. The increased frequency is about 7 Hz, i.e. twice that of trace (a). This is because there is a 2:1 entrance block at the pacemaker boundary. The burst is followed by another burst following the same mechanism. Trace (c) shows the transmembrane signal in the weakly coupled region which is reminiscent of experimentally reported EAD-like action potentials.

The modulation of action potential amplitude and oscillation of the membrane potential characteristic of EAD occurs in a large part of the medium (see Fig. 3) within the reduced coupling area and corresponds to the area swiped by the spiral core. This is not a coincidence: It is well established that the action potential amplitude in a spiral core is reduced[30] and as the spiral drifts, so does the area of reduced action potential amplitude. As the core approaches the recording site, one should see reduction in the amplitude transmembrane potential. The amplitude recovers after the core passes the recording site and moves away.

A comparison of voltage and intracellular calcium signals in Panels a and b shows that calcium overload is not involved in the genesis of action potential amplitude modulation. In fact, the first action potentials in traces (a) and (b) start from resting state, without calcium overload, yet they both develop EAD-like action potentials. On the other hand, the third-last beat in trace (a) is initiated, while intracellular calcium concentration is high; yet, this does not lead to an EAD-like action potential. In summary, calcium overload and EAD-like action potential occur independently from each other in this model.

One of the key elements of the above described bursting mechanism is the conduction block at the transition from low to high conductivity. Such block requires a steep gradient in coupling at the transition area as well as significant difference of absolute values of g_{max} and g_{min} (impedance mismatch). When either of these conditions is not met, block does not occur and reentry is not formed. Our model shows that vagal stimulation can promote bursting not only by reducing the sinus frequency but also by enhancing the impedance mismatch. Figure 4A shows wave propagation from a region of reduced coupling to a region of normal coupling in the absence of vagal stimulation. Compared to Fig. 2, the heterogeneity has been chosen smaller

to avoid block at the transition, although there still is a significant propagation delay at the interface. With vagal stimulation (Panel B, implemented as a doubling of the g_{K1} current), block occurs.

The mechanism of block enhancement by vagal stimulation is related to the increase of the excitation threshold and the reduction of the safety factor of propagation. Specifically, the increase in g_{K1} reduces the critical conductivity ratio g_{min}/g_{max}, at which unidirectional block at the interface occurs (see Figure 5A). Doubling I_{K1} reduces the critical ratio by about 20% (from 3.7 to 3) and doubling it again reduces it by another 10% (to 2.6). This demonstrates that vagal stimulation strongly promotes the induction of block in our model.

While conduction block is an essential ingredient of our bursting mechanism, a spiral wave will only develop if the line of block is sufficiently long. In Figure 5B we show that the lower the conductivity g_{min} in the reduced coupling region is, the shorter is the line of block that is needed for the induction of a spiral wave. Indeed, as g_{min} goes to zero, the critical block length is reduced in an approximately linear fashion. This makes the distal part of PVs with the lowest density of myocardial cells the most likely area where this condition is met.

Further simulations showed that the natural distribution in ion channel densities in the PVs may play a protective role against the induction of spiral waves via the described above mechanism. Figure 6 shows that when we include the normal physiological variability of ion channel densities in our model (as specified in the Methods section), spirals are significantly harder to induce and they are less stable. Panel A shows action potentials for distal-PV channel densities, atrial channel densities, and an intermediate case based on the established values for atrial tissue and PV tissue[31]. The important difference between these action potentials is that repolarization is severely delayed for distal-PV channel densities, and to a smaller degree for the intermediate case. Panel B shows, the propagation of the ectopic beat in the presence of such ion channel distribution. In this case, the unidirectional block is formed as in figure 2B-C. However, the wave fails to reenter the low conductance area.

Discussion

We demonstrated in a computer model that the combination of heterogeneous conduction in the PVs and the presence of a latent pacemaker can explain the onset of atrial fibrillation in a way that is consistent with currently available experimental results. The mechanism we demonstrated is that when the activation frequency of the heart drops below that of the ectopic pacemaker, it can induce spiral wave reentry. The model explains how AF can be triggered by a drop in heart rate, how paroxysmal bursts of activation during bradycardia produce EAD-like action potentials in the PV region, and why increased vagal tonus facilitates bursting. We further showed that the different ionic current densities present in the PVs make the induction of spiral waves in the PVs significantly harder.

The proposed mechanism is different from previous models of reentry initiation[32] that relied on well-timed extra stimuli to induce reentry. In particular, it explains in a natural way how atrial fibrillation can occur at normal heart rates or during bradycardia or pause, as it is often observed clinically[33;34]. Our studies also shed a new light onto the role of vagal stimulation in promoting the induction of AF. The arrhythmogenicity of vagal stimulation is usually attributed to the shortening of the refractory period of atrial myocytes and to increased spatial heterogeneity of refractory periods[35;36]. Yet, the effects of vagal stimulation on the refractory period do not explain the onset of fibrillation after a pause or reduction in pacing rate, reported in clinical conditions[33;34]. Our theory readily resolves this contradiction. According to our mechanisms, the vagally related slowing of the sinus rhythm unmasks any present latent pacemaker, while the amplification of the I_{K1} current by acetylcholine facilitates the block due

source-sink mismatch (see Figs. 4 and 5). Additionally, an increased I_{K1} significantly shortens the action potential, which facilitates the closure of a reentry loop[19;37] and shortens the rotation period of the spiral wave giving rise to high-frequency bursts.

An alternative explanation of high-frequency bursts in PVs is built upon EADs, action potentials with unusually long oscillatory plateau phase that can occur at slow pacing rates in some pathological conditions. EADs are usually related to Ca overload and a reduction of potassium currents[38-40]. The EAD-like potentials have been observed experimentally in PVs and were implicated as a primary cause of high frequency bursts in PVs[19;41]. While the EAD hypothesis sounds attractive due to its simplicity, it does not explain why vagal stimulation and acetylcholine release would by any means facilitate the EAD initiation. Neither has it explained the high bursting frequencies which are characteristic of reentry mechanisms and have not been reported for any types of abnormal automaticity in cardiac tissues.

It is interesting that our model also produces EAD-like potentials, yet their origin is significantly different from the conventional EAD mechanism. In our model, these EAD-like potentials occur because the action potential amplitude is severely reduced close to the tip of a spiral wave. As the spiral tip moves, different parts of the medium exhibit oscillating AP plateaus, and over time, they occur in a large part of the medium. A similar phenomenon has previously been described for spiral waves in the ventricles[42]. Explaining oscillating AP plateaus as the passing core of a spiral wave is an approach fundamentally different from the existing ones that explain as EADs caused by calcium overload, and we will now show that our approach also naturally explains the known effects of vagal stimulation.

The main assumptions of our model of AF initiation are consistent with experimental observations. Ectopic pacemakers have been reported by several studies[14;43;44] and heterogeneity in conduction in the PVs is well established12;13. Optical mapping experiments12 also report fractionated and heterogeneous conduction in the PVs which is consistent with our model postulates. A recent study[45] showed that in two thirds of bursting events, there was a long pause (the interval between sequential excitations increased by more than a factor of two) preceding the bursts. This finding fits very well with our proposed induction mechanism, since the long pause is necessary to give the ectopic pacemaker time to escape (avoid resetting by a normal sinus wave) and initiate reentry. The authors of the above study[46] did not find evidence that busting in their experiments was caused by reentry, but this may be because they were not mapping the most distal part of the pulmonary veins with sufficient spatial resolution.

The proposed mechanism may work for much shorter lines of blocks than discussed in this paper. While we here considered block induced by heterogeneous conduction along a line of about 12 mm length (corresponding to a PV with a diameter of about at least 7 mm), the same mechanism would work in much smaller regions if the conduction velocity is proportionally reduced. Since propagation velocities below 5 cm/s have been observed in the PV[13], micro-reentry appears to be a real possibility. This is the reason that we formulated our model with no-flux boundary conditions, which allows us to interpret our simulations on different space scales. The fact that we chose a diagonal, isotropic conductivity tensor does not pose a significant limitation because source-sink mismatch and unidirectional block can equally be achieved with non-diagonal, anisotropic conductivities tensors. The reason we chose the conductivity tensor diagonal and isotropic was only to keep the discussion simple. A similar mechanism of bradycardic onset of spiral wave reentry has been described for ventricular tissue47, which suggests that this mechanism is not sensitive to details of the ionic model used.

Heterogeneous refractoriness, an arrhythmia mechanism similar to heterogeneous conductivity, does not seem to be a possible cause for unidirectional block in our case. Indeed,

the ectopic pacemaker in the pulmonary veins activates later than the sinus node would have at its normal rate, so any beat coming from the ectopic pacemaker should encounter all cells fully recovered from refractory state.

Our study demonstrates that the pattern of ion channel protein expression[31] in the PV and the resulting ion channel densities[26] do not favor the initiation of a spiral wave. The increase in resting membrane expression and reduction in I_{K1}[26] causes an increase in the refractive period of PV myocytes and reduces the probability of reentry. This may represent an evolutionary mechanism protecting against arrhythmia induction in the PVs. The proximity of a latent pacemaker to a fairly special heterogeneity in electrical coupling, required by our mechanism for AF initiation, is also difficult to meet, which explains why the great majority of hearts is not prone to AF. While the reasons outlined above make the proposed mechanism attractive from the evolutional prospective, they also make its experimental verification in animal models difficult, because it will probably occur quite rarely.

The described above model of bursting in pulmonary veins may have multiple clinical implications. If verified, it can allow a more efficient way of provoking atrial fibrillation in the operating room which will enable a more precise identification of targets for radiofrequency ablation thus increasing efficacy of anti-arrhythmic therapies.

Acknowledgments

Research for this article was supported by NIH grants RO1-HL071762-01A1 and ROI-HL071635-01.

Reference List

1. Go AS, Hylek EM, Phillips KA, Chang Y, Henault LE, Selby JV, Singer DE. Prevalence of diagnosed atrial fibrillation in adults: national implications for rhythm management and stroke prevention: the AnTicoagulation and Risk Factors in Atrial Fibrillation (ATRIA) Study. JAMA 2001;285:2370–5. [PubMed: 11343485]
2. Dorian P, Jung W, Newman D, Paquette M, Wood K, Ayers GM, Camm J, Akhtar M, Luderitz B. The impairment of health-related quality of life in patients with intermittent atrial fibrillation: implications for the assessment of investigational therapy. J Am Coll Cardiol 2000;36:1303–9. [PubMed: 11028487]
3. Prystowsky EN, Benson DW, Fuster V, Hart RG, Kay GN, Myerburg RJ, Naccarelli GV, Wyse DG. Management of patients with atrial fibrillation. A Statement for Healthcare Professionals. From the Subcommittee on Electrocardiography and Electrophysiology, American Heart Association. Circulation 1996;93:1262–77. [PubMed: 8653857]
4. Wijffels MC, Kirchhof CJ, Dorland R, Allessie MA. Atrial fibrillation begets atrial fibrillation. A study in awake chronically instrumented goats. Circulation 1995;92:1954–68. [PubMed: 7671380]
5. Saksena S, Hettrick DA, Koehler JL, Grammatico A, Padeletti L. Progression of paroxysmal atrial fibrillation to persistent atrial fibrillation in patients with bradyarrhythmias. Am Heart J 2007;154:884–92. [PubMed: 17967594]
6. Jais P, Haissaguerre M, Shah DC, Chouairi S, Gencel L, Hocini M, Clementy J. A focal source of atrial fibrillation treated by discrete radiofrequency ablation. Circulation 1997;95:572–6. [PubMed: 9024141]
7. Chen YJ, Chen SA. Electrophysiology of pulmonary veins. J Cardiovasc Electrophysiol 2006;17:220–4. [PubMed: 16533265]
8. Haissaguerre M, Jais P, Shah DC, Takahashi A, Hocini M, Quiniou G, Garrigue S, Le Mouroux A, Le Metayer P, Clementy J. Spontaneous initiation of atrial fibrillation by ectopic beats originating in the pulmonary veins. N Engl J Med 1998;339:659–66. [PubMed: 9725923]
9. Tsai CF, Tai CT, Hsieh MH, Lin WS, Yu WC, Ueng KC, Ding YA, Chang MS, Chen SA. Initiation of atrial fibrillation by ectopic beats originating from the superior vena cava: electrophysiological

characteristics and results of radiofrequency ablation. Circulation 2000;102:67–74. [PubMed: 10880417]

10. Patterson E, Jackman WM, Beckman KJ, Lazzara R, Lockwood D, Scherlag BJ, Wu R, Po S. Spontaneous pulmonary vein firing in man: relationship to tachycardia-pause early afterdepolarizations and triggered arrhythmia in canine pulmonary veins in vitro. J Cardiovasc Electrophysiol 2007;18:1067–1075. [PubMed: 17655663]
11. Saito T, Waki K, Becker AE. Left atrial myocardial extension onto pulmonary veins in humans: anatomic observations relevant for atrial arrhythmias. J Cardiovasc Electrophysiol 2000;11:888–94. [PubMed: 10969751]
12. Arora R, Verheule S, Scott L, Navarrete A, Katari V, Wilson E, Vaz D, Olgin JE. Arrhythmogenic substrate of the pulmonary veins assessed by high-resolution optical mapping. Circulation 2003;107:1816–21. [PubMed: 12665495]
13. Hocini M, Ho SY, Kawara T, Linnenbank AC, Potse M, Shah D, Jais P, Janse MJ, Haissaguerre M, De Bakker JM. Electrical conduction in canine pulmonary veins: electrophysiological and anatomic correlation. Circulation 2002;105:2442–8. [PubMed: 12021234]
14. Brunton TL, Fayrer J. Note on independent pulsation of the pulmonary veins and Vena Cava. Proceedings of the Royal Society of London 1876;25:174–176.
15. Cheung DW. Electrical activity of the pulmonary vein and its interaction with the right atrium in the guinea-pig. J Physiol 1981;314:445–456. [PubMed: 7310698]
16. Chen YJ, Chen SA, Chang MS, Lin CI. Arrhythmogenic activity of cardiac muscle in pulmonary veins of the dog: implication for the genesis of atrial fibrillation. Cardiovasc Res 2000;48:265–73. [PubMed: 11054473]
17. Chen YC, Chen SA, Chen YJ, Chang MS, Chan P, Lin CI. Effects of thyroid hormone on the arrhythmogenic activity of pulmonary vein cardiomyocytes. J Am Coll Cardiol 2002;39:366–72. [PubMed: 11788233]
18. Chen YJ, Chen SA, Chen YC, Yeh HI, Chan P, Chang MS, Lin CI. Effects of rapid atrial pacing on the arrhythmogenic activity of single cardiomyocytes from pulmonary veins: implication in initiation of atrial fibrillation. Circulation 2001;104:2849–54. [PubMed: 11733406]
19. Patterson E, Po SS, Scherlag BJ, Lazzara R. Triggered firing in pulmonary veins initiated by in vitro autonomic nerve stimulation. Heart Rhythm 2005;2:624–31. [PubMed: 15922271]
20. Osterrieder W, Noma A, Trautwein W. On the kinetics of the potassium channel activated by acetylcholine in the S-A node of the rabbit heart. Pflugers Arch 1980;386:101–109. [PubMed: 6253873]
21. Dexter F, Saidel GM, Levy MN, Rudy Y. Mathematical model of dependence of heart rate on tissue concentration of acetylcholine. Am J Physiol 1989;256:H520–H526. [PubMed: 2916685]
22. Volders PG, Vos MA, Szabo B, Sipido KR, de Groot SH, Gorgels AP, Wellens HJ, Lazzara R. Progress in the understanding of cardiac early afterdepolarizations and torsades de pointes: time to revise current concepts. Cardiovasc Res 2000;46:376–392. [PubMed: 10912449]
23. Zeng J, Laurita KR, Rosenbaum DS, Rudy Y. Two components of the delayed rectifier K+ current in ventricular myocytes of the guinea pig type. Theoretical formulation and their role in repolarization. Circ Res 1995;77:140–152. [PubMed: 7788872]
24. Silva J, Rudy Y. Subunit interaction determines IKs participation in cardiac repolarization and repolarization reserve. Circulation 2005;112:1384–1391. [PubMed: 16129795]
25. Ramirez RJ, Nattel S, Courtemanche M. Mathematical analysis of canine atrial action potentials: rate, regional factors, and electrical remodeling. Am J Physiol Heart Circ Physiol 2000;279:1767–85.
26. Ehrlich JR, Cha TJ, Zhang L, Chartier D, Melnyk P, Hohnloser SH, Nattel S. Cellular electrophysiology of canine pulmonary vein cardiomyocytes: action potential and ionic current properties. J Physiol 2003;551:801–13. [PubMed: 12847206]
27. Kneller J, Zou R, Vigmond EJ, Wang Z, Leon LJ, Nattel S. Cholinergic atrial fibrillation in a computer model of a two-dimensional sheet of canine atrial cells with realistic ionic properties. Circ Res 2002;90:E73–E87. [PubMed: 12016272]
28. Kneller J, Zou R, Vigmond EJ, Wang Z, Leon LJ, Nattel S. Cholinergic atrial fibrillation in a computer model of a two-dimensional sheet of canine atrial cells with realistic ionic properties. Circ Res 2002;90:E73–E87. [PubMed: 12016272]

29. Kneller J, Zou R, Vigmond EJ, Wang Z, Leon LJ, Nattel S. Cholinergic atrial fibrillation in a computer model of a two-dimensional sheet of canine atrial cells with realistic ionic properties. Circ Res 2002;90:E73–E87. [PubMed: 12016272]
30. Pertsov AM, Davidenko JM, Salomonsz R, Baxter WT, Jalife J. Spiral waves of excitation underlie reentrant activity in isolated cardiac muscle. Circ Res 1993;72:631–650. [PubMed: 8431989]
31. Melnyk P, Ehrlich JR, Pourrier M, Villeneuve L, Cha TJ, Nattel S. Comparison of ion channel distribution and expression in cardiomyocytes of canine pulmonary veins versus left atrium. Cardiovasc Res 2005;65:104–16. [PubMed: 15621038]
32. Po SS, Li Y, Tang D, Liu H, Geng N, Jackman WM, Scherlag B, Lazzara R, Patterson E. Rapid and stable re-entry within the pulmonary vein as a mechanism initiating paroxysmal atrial fibrillation. J Am Coll Cardiol 2005;45:1871–7. [PubMed: 15936621]
33. Dimmer C, Szili-Torok T, Tavernier R, Verstraten T, Jordaens LJ. Initiating mechanisms of paroxysmal atrial fibrillation. Europace 2003;5:1–9. [PubMed: 12504634]
34. Schwartzman D, Blagev DP, Brown ML, Mehra R. Electrocardiographic events preceding onset of atrial fibrillation: insights gained using an implantable loop recorder. J Cardiovasc Electrophysiol 2006;17:243–6. [PubMed: 16643393]
35. ALESSI R, NUSYNOWITZ M, ABILDSKOV JA, Moe GK. Nonuniform distribution of vagal effects on the atrial refractory period. Am J Physiol 1958;194:406–410. [PubMed: 13559489]
36. Ninomiya I. Direct evidence of nonuniform distribution of vagal effects on dog atria. Circ Res 1966;19:576–583. [PubMed: 5925156]
37. Scherlag BJ, Patterson E, Po SS. The neural basis of atrial fibrillation. J Electrocardiol 2006;39:180–3. [PubMed: 16580416]
38. Volders PG, Vos MA, Szabo B, Sipido KR, de Groot SH, Gorgels AP, Wellens HJ, Lazzara R. Progress in the understanding of cardiac early afterdepolarizations and torsades de pointes: time to revise current concepts. Cardiovasc Res 2000;46:376–392. [PubMed: 10912449]
39. Zeng J, Laurita KR, Rosenbaum DS, Rudy Y. Two components of the delayed rectifier K+ current in ventricular myocytes of the guinea pig type. Theoretical formulation and their role in repolarization. Circ Res 1995;77:140–152. [PubMed: 7788872]
40. Silva J, Rudy Y. Subunit interaction determines IKs participation in cardiac repolarization and repolarization reserve. Circulation 2005;112:1384–1391. [PubMed: 16129795]
41. Chen YJ, Chen SA, Chang MS, Lin CI. Arrhythmogenic activity of cardiac muscle in pulmonary veins of the dog: implication for the genesis of atrial fibrillation. Cardiovasc Res 2000;48:265–73. [PubMed: 11054473]
42. Pertsov AM, Davidenko JM, Salomonsz R, Baxter WT, Jalife J. Spiral waves of excitation underlie reentrant activity in isolated cardiac muscle. Circ Res 1993;72:631–650. [PubMed: 8431989]
43. Cheung DW. Electrical activity of the pulmonary vein and its interaction with the right atrium in the guinea-pig. J Physiol 1981;314:445–456. [PubMed: 7310698]
44. Chen YJ, Chen SA, Chang MS, Lin CI. Arrhythmogenic activity of cardiac muscle in pulmonary veins of the dog: implication for the genesis of atrial fibrillation. Cardiovasc Res 2000;48:265–73. [PubMed: 11054473]
45. Patterson E, Jackman WM, Beckman KJ, Lazzara R, Lockwood D, Scherlag BJ, Wu R, Po S. Spontaneous pulmonary vein firing in man: relationship to tachycardia-pause early afterdepolarizations and triggered arrhythmia in canine pulmonary veins in vitro. J Cardiovasc Electrophysiol 2007;18:1067–1075. [PubMed: 17655663]
46. Patterson E, Jackman WM, Beckman KJ, Lazzara R, Lockwood D, Scherlag BJ, Wu R, Po S. Spontaneous pulmonary vein firing in man: relationship to tachycardia-pause early afterdepolarizations and triggered arrhythmia in canine pulmonary veins in vitro. J Cardiovasc Electrophysiol 2007;18:1067–1075. [PubMed: 17655663]
47. Zemlin CW, Pertsov AM. Bradycardic onset of spiral wave re-entry: structural substrates. Europace 9:vi59–vi63. [PubMed: 17959694]

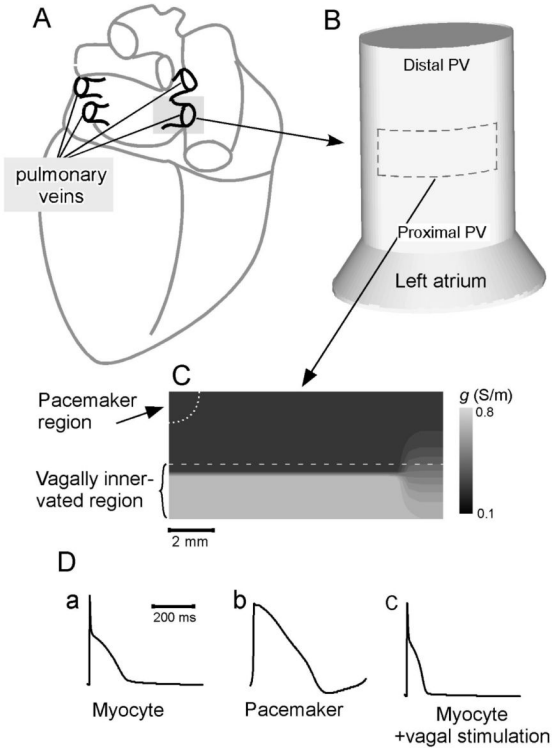

Figure 1.

Simulation of electrical propagation in the myocardial sleeves. **A:** Location of the pulmonary veins in the left atrium of the heart. **B:** A single pulmonary vein (marked in Panel A) Dashed rectangle shows the approximate location of the simulated region (see Panel C) **C:** Spatial distribution of electrophysiological properties in our model. Gray levels indicate the local conductivity (the conductivity tensor g is isotropic, $g_x(x,y)=g_y(x,y)$). Dashed line indicates the boundary of vagally innervated tissue. Dotted line marks the pacemaker region. **D:** Action potentials from different cell types.

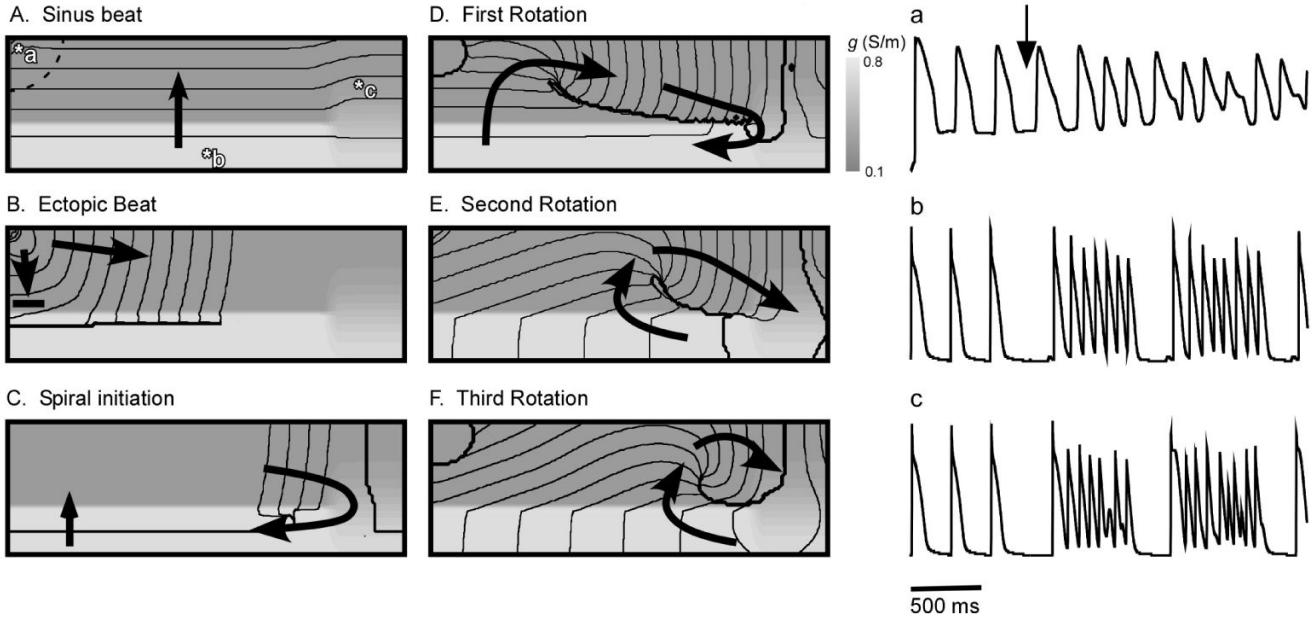

Figure 2.

Bursting in the pulmonary veins triggered by a sudden reduction in heart rate. **A-F:** Initiation of a spiral wave by an ectopic beat originating in the pacemaker region. Black lines are isochrones, spaced 5 ms apart, arrows indicate the direction of wave propagation. **A:** Sinus activation. **B:** Ectopic wave originated in the pacemaker region is blocked at the interface of the areas with reduced (medium gray) and normal (light gray) coupling . **C:** The ectopic beat penetrates into the normally conducting region, collides with the next sinus front, and reenters the low conduction region (upward arrow) forming a spiral wave. **D-F**: Subsequent evolution of the spiral wave. **a-c:** Transmembrane voltage signal at three different locations (marked in Panel A). Three sinus stimulations, followed by two high-frequency bursts. Bursting starts after a slowdown in the pacing rate from 500 ms to 800 ms.

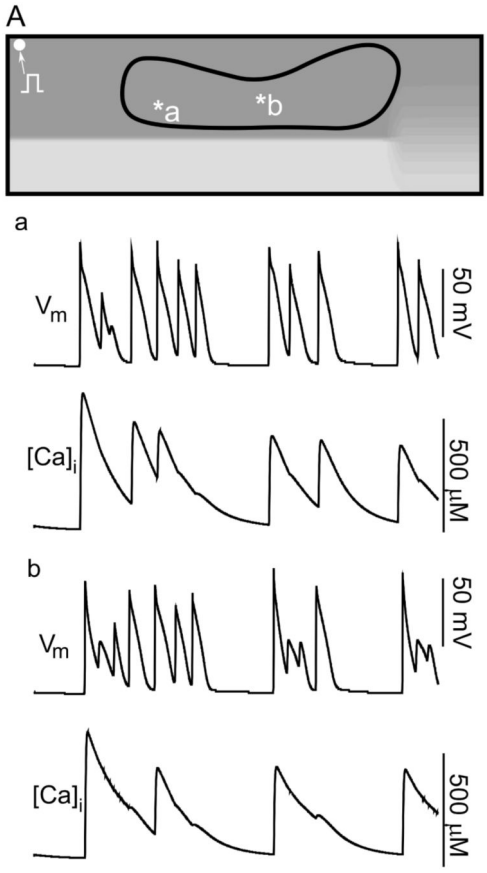

Figure 3.
Action potentials resembling early afterdepolarizations (EADs) during spiral wave reentry in the pulmonary veins. **A:** Area in which EAD-like APs occur. **a-b:** Electrical and intracellular calcium signals recorded from the points marked in the upper Panel.

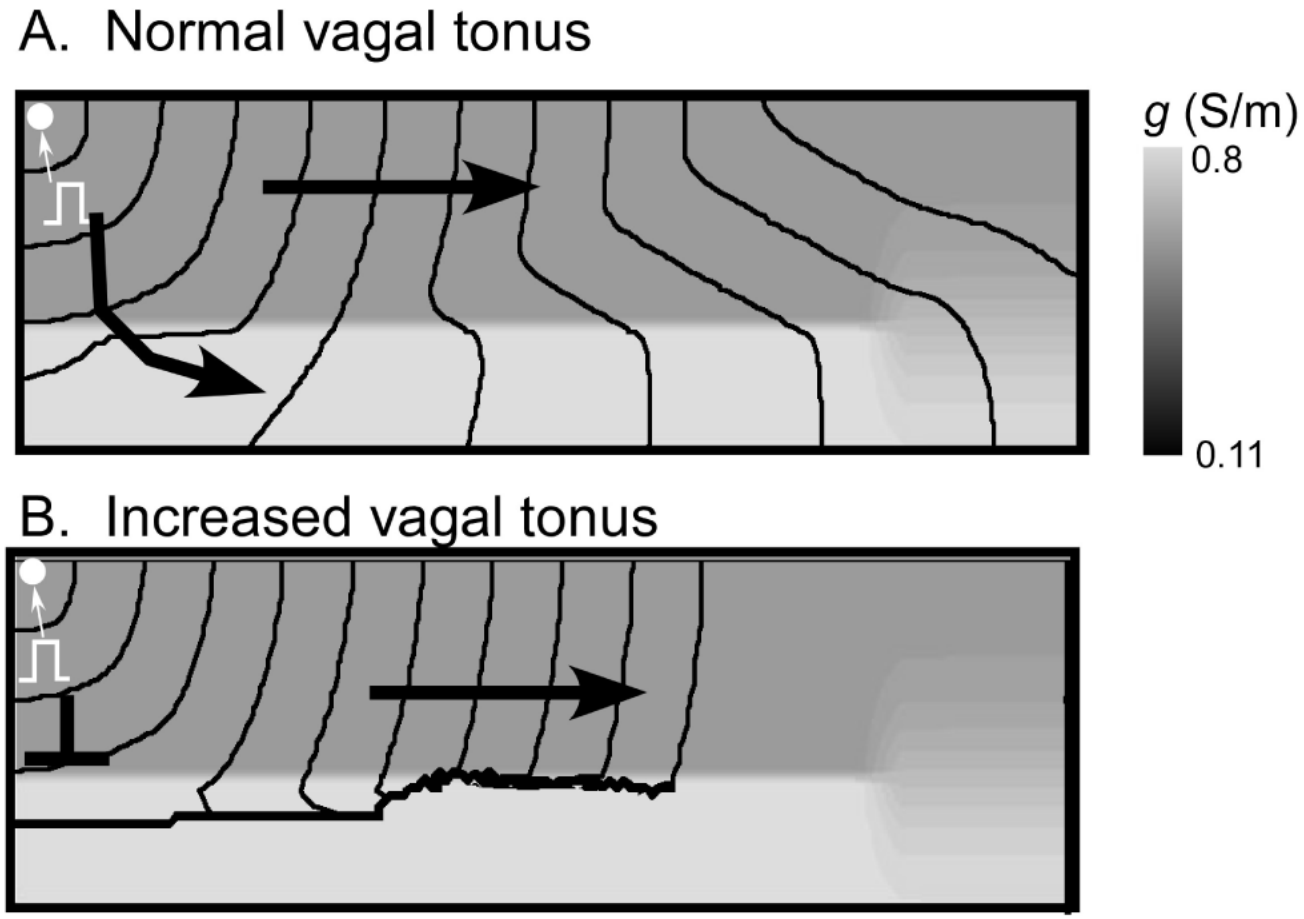

Figure 4.
Vagal stimulation induces conduction block at coupling heterogeneities. **A:** Propagation during normal vagal tonus. For g_{min}=0.11 and Δg=0.69, a wave initiated in the distal end penetrates into the proximal PV. **B:** Increased vagal tonus, modeled by doubling I_{K1}, leads to conduction block at the interface between normal and reduced conduction.

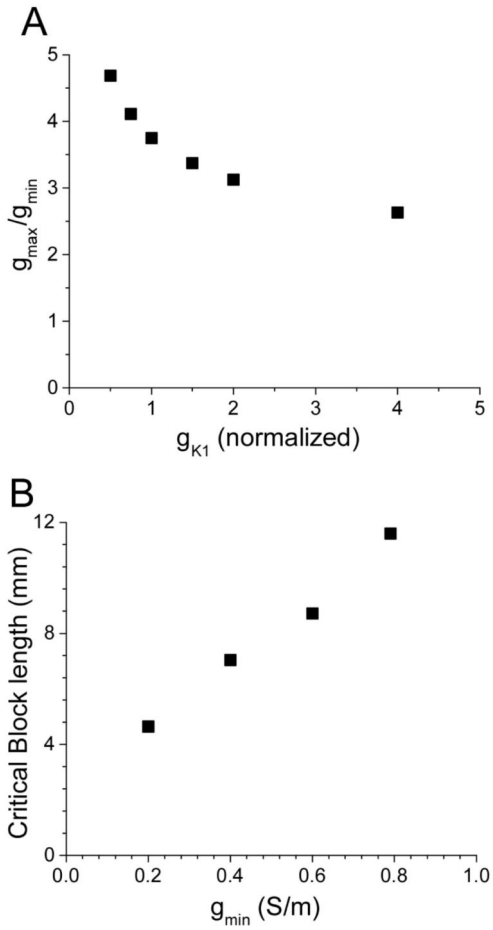

Figure 5.
Conditions needed for spiral reentry induction. **A:** Dependence of the critical ratio g_{max} / g_{min}, at which block occurs, on g_{K1}. **B:** Dependence of critical block length on g_{min} (g_{max} was kept constant).

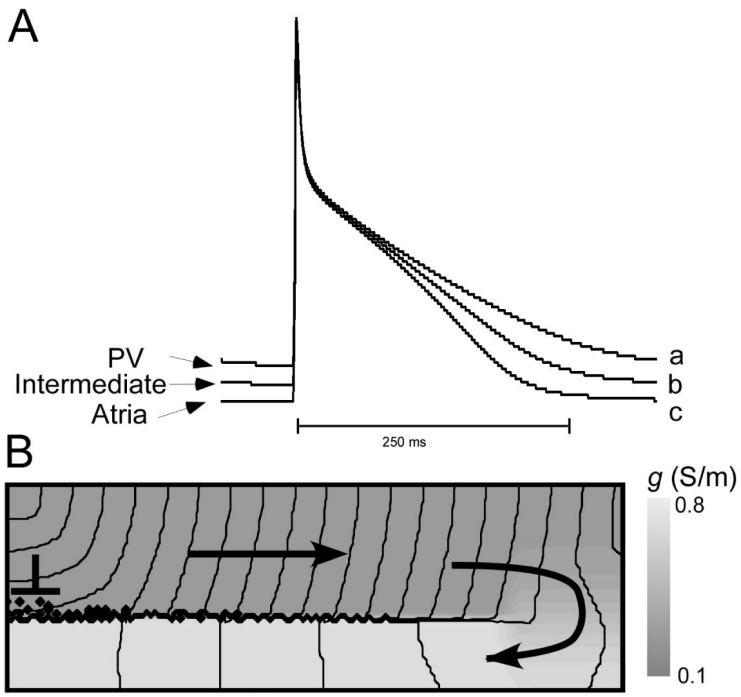

Figure 6.

The natural distribution of ion channel densities. Reentry induction is inhibited for a. **A:** Action potentials for ion channel densities typical in the PV region, the atria, and densities halfway between these two cases. **B:** The first stimulus applied to the distal PV does not produce reentry.